Enzymatic- and Light-Degradable Hybrid Nanogels: Crosslinking of Polyacrylamide with Acrylate-Functionalized Dextrans Containing Photocleavable Linkers

Daniel Klinger, Katharina Landfester

Max Planck Institute for Polymer Research, Ackermannweg 10, 55128 Mainz, Germany
Correspondence to: K. Landfester (E-mail: landfester@mpip-mainz.mpg.de)

Received 4 November 2011; accepted 7 November 2011; published online 28 November 2011
DOI: 10.1002/pola.25845

ABSTRACT: Enzymatically cleavable and light-degradable hybrid nanogels were prepared by free radical inverse miniemulsion copolymerization of acrylamide (AAm) with a newly synthesized functional dextran crosslinker containing acrylate moieties attached to the backbone via a photolabile linker, that is, dextran-photolabile linker-acrylate (Dex-PL-A). The Dex-PL-A/AAm feed ratio was systematically varied to investigate the influence of the particle composition on the gel properties. The resulting hydrogel nanoparticles were examined with regard to their degradation behavior upon the appliance of the two orthogonal stimuli by turbidity measurements in combination with dynamic light scattering. Although continuous photolytic cleavage of the photolabile linkers between polyacrylamide chains and dextran molecules was found to proceed fast and quantitatively yielding completely disintegrated networks, stepwise irradiation resulted in partial degradation of crosslinking points. Thus, nanogels of a desired specific degree of swelling (DGS) can be obtained by adjusting the irradiation time accordingly. Partial enzymatic cleavage of the dextran backbones of the Dex-PL-A crosslinking molecules resulted in an increase in the DGS of the nanogels up to a constant value. Subsequent irradiation of those swollen hydrogel particles was used to fully degrade the network structure in a second step. Hence, a two-step degradation profile was realized by the combination of the two orthogonal stimuli. © 2011 Wiley Periodicals, Inc. J Polym Sci Part A: Polym Chem 50: 1062–1075, 2012

KEYWORDS: biopolymers; crosslinking; degradation; enzymes; microgels; photochemistry; swelling

INTRODUCTION Nanogels as particulate structures in the submicron size range consist of chemically or physically intermolecularly crosslinked (hydrophilic) networks, which are swollen in a suitable solvent. They represent a highly interesting class of materials because they combine the characteristics of macroscopic hydrogels (e.g., structural integrity in combination with fluid-like transport characteristics) with those of colloidal dispersions (e.g., good colloidal stability, facile synthesis, and control over particle size).[1,2] Stimuli-responsive micro- or nano-gels exhibit a response of their respective network structure to changes in the (chemical) environment thus rendering those materials "smart." This behavior gives rise to a broad variety of applications including the fields of drug or gene delivery, chemical sensing, triggered catalysis, and optics.[1,2]

On one hand, a response to a specific stimulus is often characterized by a change in the physicochemical parameters of the network resulting in a variation of the degree of swelling (DGS). Realization of this concept is achieved by the incorporation of functional stimuli-responsive moieties into the gel-forming polymers.[3,4] The resulting reversible volume phase transition is governed by an imbalance between repulsive and attractive forces acting in the particles and can be influenced by different triggers such as pH,[5,6] temperature,[7,8] or ionic strength.[9]

On the other hand, the incorporation of labile crosslinking points is a different approach to stimuli-responsive gel particles. In this case, the triggered degradation of the crosslinking molecules leads to the disintegration of the network structure yielding freely soluble polymer chains. Such degradable nanogels offer the potential to release entrapped compounds from the network upon the appliance of an external trigger. Here, an initial mesh size of the gel smaller than the hydrodynamic diameter of the respective substance to be released prevents diffusion from the gel until triggered cleavage of crosslinking points increases the pore sizes resulting in the release.[3,10] This characteristic cannot only be applied to release applications; a triggered accessibility of, for example, catalytic substances (metal nanoparticles, enzymes) is imaginable and of high interest in materials science. Investigated approaches to realize the described concept are based on, for example, pH-sensitive crosslinkers

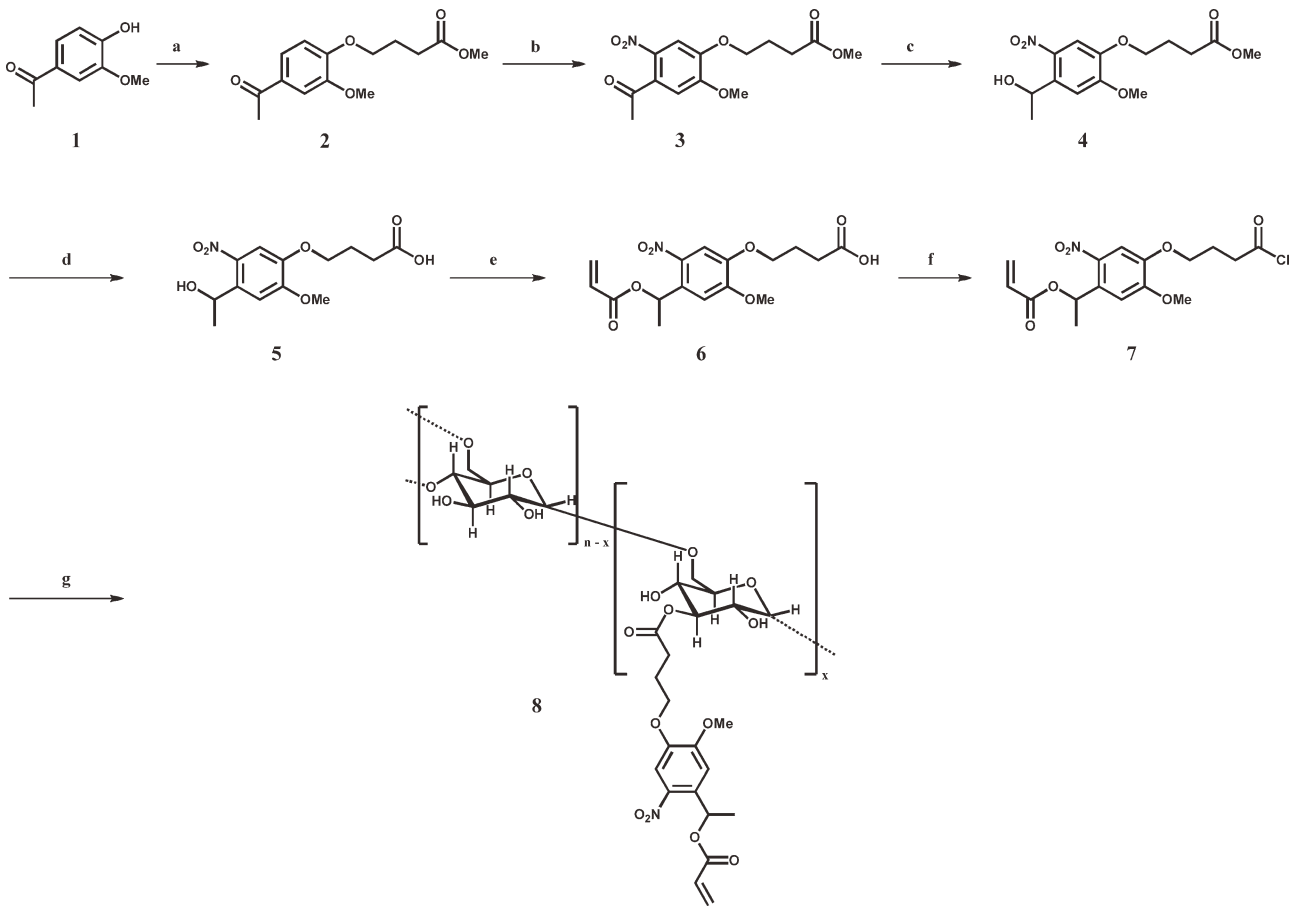

SCHEME 1 Synthetic pathway to Dex-PL-A. Reagents and conditions: (a) methyl-4-bromobutyrate, K_2CO_3/DMF (anhyd.), 25 °C, 16 h, quant.; (b) acetic anhydride/nitric acid (1:2, v/v), 0 °C, 3 h, 53%; (c,d) $NaBH_4$/MeOH/THF, 25 °C, 16 h, NaOH, 25 °C, 7 h, 89%; (e) acryloyl chloride, NEt_3, DCM, 0 °C to RT, 16 h, 65%; (f) oxalyl chloride, DMF (cat.), DCM (anhyd.), 3 h, quant.; (g) detxtran (6k), NEt_3, LiCl, DMF (anhyd.), RT, 16 h, 60 °C, 1 h, 58%.

containing various acid-labile moieties such as tertiary esters or acetals for the preparation of degradable microgels in both aqueous[11,12] and organic media.[13]

An alternative concept of degradable (micro-)gels focuses on the utilization of dextrans as naturally occurring polysaccharides, which can be cleaved upon the incubation with dextranase. Covalent functionalization of dextran chains with either polymerizable vinyl groups[14,15] or thermal initiators[16] enables the formation of hydrogels by free radical (co)polymerization in aqueous solutions.[17] The resulting networks can then be degraded by the addition of dextranase, thus enabling the release of embedded active compounds.[18] Enzymatically degradable microgels for the delivery of immunoglobulin G as a model protein were prepared in the group of Hennink by the simultaneous embedding of the protein and dextranase into the network.[19]

Regarding the versatility of such delivery systems, the ability to respond to multiple orthogonal triggers is generally of high interest. In this context, the concept of degradable microgels based on dextran as crosslinkers was further developed by introducing a hydrolytically labile spacer between the polymerizable vinyl groups and the enzymatically degradable dextran chain.[20,21] The resulting microgels were shown to be degradable due to the hydrolysis of the labile spacer bonds under either basic or acidic conditions.[22] The combination of these microgels with a semipermeable shell structure finally led to self-exploding capsules as a very interesting new delivery system.[23] Here, hydrolysis of the degradable microgel core is accompanied by the diffusion of solvent into the core, thus creating a pressure in the capsule which finally leads to a burst of the membrane and the release of compounds from the interior.

Concerning either degradation- or swelling-induced release systems based on enzymatic or pH-sensitive materials both require the addition of protons/enzymes or the localization of the carrier system in specific milieus. In comparison, the release of a payload upon applying an external trigger without a change in the chemical composition of the surrounding media bears the advantage of an on-demand delivery. Among different stimuli fulfilling this criterion, light represents an outstanding position because it offers the possibility to change the network properties in very confined spaces and time scales. Furthermore, it can be applied in a very precise manner by selecting suitable wavelengths,

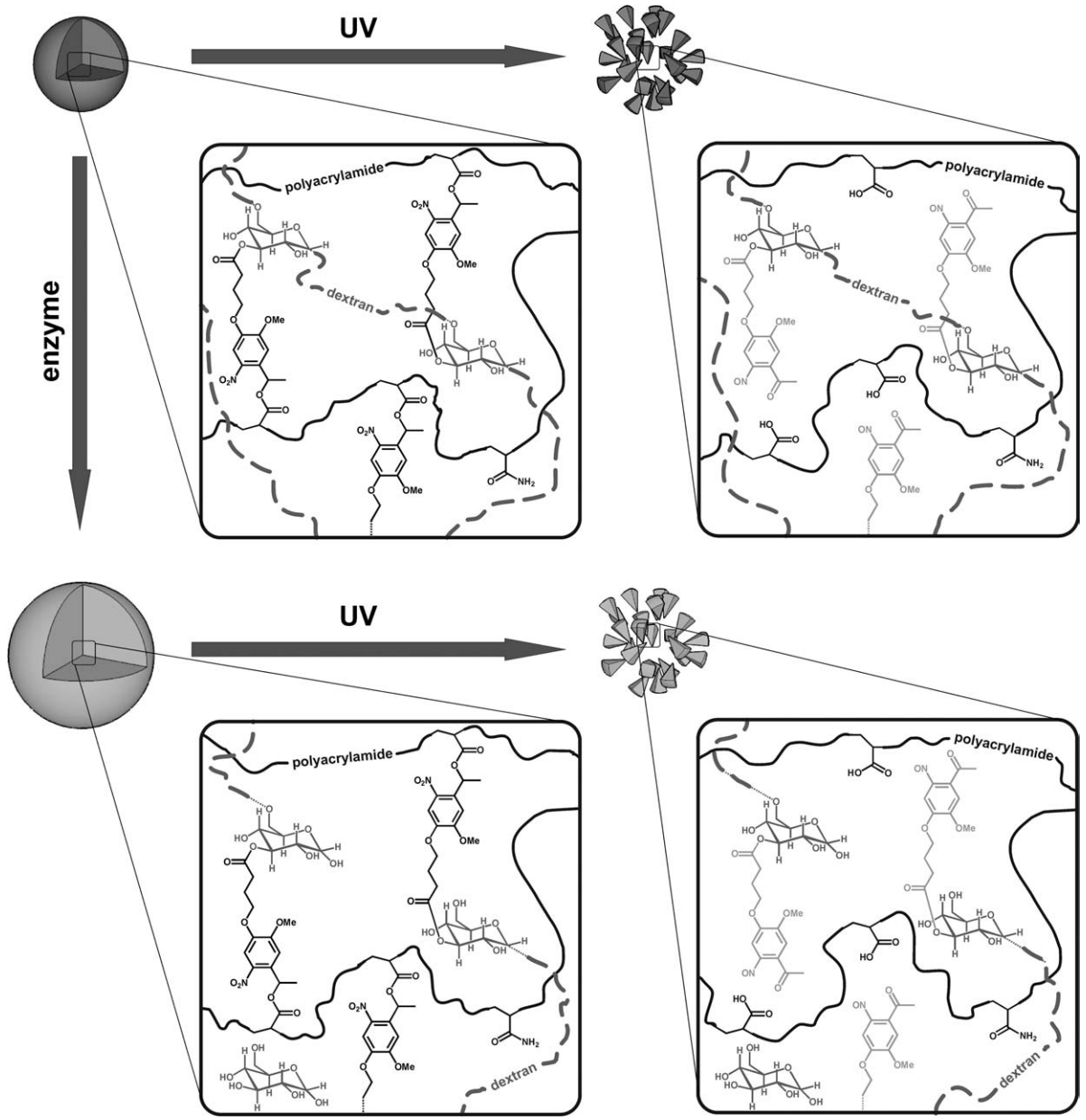

FIGURE 1 Schematic representation of the stimuli-induced degradation of hybrid p(AAm-*co*-Dex-PL-A) nanogels.

polarization directions, and intensities in a noncontact approach. The concept of light cleavable crosslinkers was recently described for the preparation of photodegradable macroscopic hydrogels by Kloxin et al.[24] Transferring this approach to the nanometer size range, the preparation of UV-degradable poly(methyl methacrylate) (PMMA) microgels has recently been reported by our group.[25]

The aim of this work is the preparation of double stimuli-responsive nanogels to be degradable upon the addition of dextranase or the irradiation with light as an orthogonal second trigger. Our approach to realize the described concept is based on free radical inverse miniemulsion copolymerization of acrylamide (AAm) with a newly synthesized functional dextran crosslinker containing acrylate moieties covalently attached to the backbone via a photolabile linker, that is, dextran-photolabile linker-acrylate (Dex-PL-A). Multiple substitution of glucopyranose units in the dextran chain with polymerizable acrylate units enables the utilization of the functionalized polysaccharide as crosslinker in the copolymerization. Enzymatic degradation of the resulting nanogels can then be achieved by cleavage of the dextran backbone upon the addition of dextranase. Even though this sensitivity depends on a change in the chemical composition of the respective surrounding media, it gives rise to a potential release of compounds in aqueous media of neutral pH, therefore representing an alternative approach to predominantly used acid-labile crosslinkers. The light sensitivity can be realized by the introduction of a photolabile linker molecule between the polymerizable acrylate units and the dextran chain. Irradiation of the resulting nanogels leads to

photolytic cleavage of the covalent linkage of the polyacrylamide (PAAm) chains to the dextran chains and is assumed to yield freely soluble polyacrylamide and dextran chains. Both stimuli can be applied either separately or subsequently, thus enabling a good and versatile control over the swelling and degradation behavior.

RESULTS AND DISCUSSION

Enzymatically and photolytically degradable hybrid nanogels were designed to alter their network structure upon appliance of two different stimuli; that is, the addition of dextranase or the irradiation with UV light. The integration of the double stimuli-responsive character can be achieved by using a dextran molecule containing radically polymerizable acrylate groups covalently bound to the polysaccharide backbone via a photolabile linker molecule (Dex-PL-A). Copolymerization with AAm in an inverse miniemulsion process leads to hybrid nanogels. Here, the functionalized Dex-PL-A molecules act as cleavable crosslinkers due to multiple acrylate moieties attached to a single dextran chain. Network degradation is based on either the enzymatic degradation of the dextran backbone or the photolytic cleavage of the covalent linkage of the polyacrylamide chains to the dextran chains as shown in Figure 1. Both stimuli can be applied either separately or subsequently, thus enabling a good and versatile control over the swelling and degradation behavior.

In general, one way to incorporate potential water soluble functional compounds into polymeric nanogels is their embedding already during the network formation.[19,22] This approach can be achieved by inverse miniemulsion copolymerization of a monomer and a crosslinker in the presence of the respective substance. A requirement, however, are water soluble monomers and crosslinkers. Regarding delivery applications, a release of the respective functional compound is generally determined by diffusion from the network and governed by the mesh size of the gel.[3] A specific molecular design of the network structure allows the incorporation of stimuli-sensitive properties, thus enabling a release controlled by external triggers. As one example, the stimuli-responsive behavior can be achieved by the utilization of labile crosslinking points. Triggered (partial) degradation of the latter leads to either highly swollen gels of increased mesh sizes or complete particle degradation, thus enabling the release of functional compounds.[11]

The newly synthesized Dex-PL-A crosslinking molecules are designed to fulfill both of the above mentioned criteria. As naturally occurring polysaccharides, dextrans are well-known for their good water solubility and their enzymatic degradability upon the treatment with dextranase.[14] Hence, the potential of network formation from aqueous solutions is combined with the degradation of the gels as a response to changes of the chemical environment; that is, the presence of dextranase. Moreover, the introduction of a photolytic cleavable linker molecule between the dextran chain and the polymerizable acrylate groups enables the gel degradation upon the appliance of light as a second trigger. Because light can be applied in a very precise manner—for example, by selecting suitable wavelengths—and in very confined spaces in a noncontact approach, it represents an orthogonal approach to the enzymatic sensitivity. In this context, *o*-nitrobenzylic esters are well-known for their good photolytic properties,[26] such as fast and quantitative reactions[27] in a broad variety of environments.[28,29]

Synthesis and Characterization of Dextran-Photolabile Linker-Acrylate

Dex-PL-A molecules were synthesized according to Scheme 1 in order to combine the enzymatic degradability of the dextran biopolymer with the photolytic properties of the *o*-nitrobenzyl ester groups in the photolabile linker between acrylate moieties and the polysaccharide backbone.

The carboxylic acid and hydroxyl functionalized photolabile chromophore (5) was synthesized according to the procedure described earlier.[25] In brief, the ether formation of (1) with methyl-4-bromobutyrate was followed by nitration of the aromatic core with acetic anhydride/nitric acid. Reduction of the keto group of (4) and subsequent ester hydrolysis yielded (5) in good yields. In a next step, the hydroxyl group was reacted with acryloyl chloride to attach the polymerizable unit through a photolabile *o*-nitrobenzyl ester bond. The carboxyl group of (5) was then activated by forming the respective carboxyloyl chloride with oxalylchloride. Finally, the crosslinking molecule Dex-PL-A (8) was obtained by the reaction of hydroxyl groups of dextran with the activated carboxyl group of (5), thus covalently attaching the acrylate moieties to the dextran backbone via the photolabile linker. The obtained crosslinker was investigated with regard to the degree of substitution (DS) by means of ^{1}H NMR measurements. Calculation of the peak area ratio of the 6 protons (aromatic, olefinic, and tertiary benzylic) of the photolabile linker to the one anomeric proton of dextran afforded a DS = 0.17. In other words, on one dextran chain consisting of ~34 glucopyranosyl groups, 5–6 of these groups are functionalized. Although a low DS is assumed to decrease the crosslinking efficiency, functionalization of the dextran with too many acrylate side groups could influence the enzymatic degradation behavior due to a reduced accessibility of the dextran backbone as a result of sterical hindrance. The medium DS of 0.17 should allow a sufficient crosslinking upon copolymerization with AAm while maintaining the enzymatic degradability.

Additionally, a comparatively low molecular weight of 6000 g/mol of the used dextran was chosen to enable a good distribution of the crosslinking points in the resulting gel. Preliminary studies performed on PAAm nanogels crosslinked with dextran methacrylates confirmed this hypothesis and are published elsewhere.[30]

Regarding the photolysis of the crosslinking molecules and the resulting nanogels, a fast and quantitative reaction under mild conditions is highly favored. The α methyl group on the benzylic carbon of the *o*-nitrobenzyl moiety was introduced into the photolabile chromophore as it is known to increase the rate of photolysis significantly.[31] By considering the abstraction of a benzylic proton by the photoactivated nitro

group as the rate limiting step in the photolysis of the *o*-nitrobenzyl group, the additional methyl group increases the acidity of this proton.

Furthermore, Norrish-type side reactions, which primarily take place for irradiations with wavelengths of $\lambda < 300$ nm, should be avoided. In this context, the introduction of alkoxy substituents in the *o*-nitrobenzylic core results in a modified electronic structure of the chromophore which is known to result in a considerably increased UV absorption for $\lambda > 315$ nm,[32] and thus allows for a more gentle decomposition with possible benefits for release applications of sensitive molecules.

Figure 2 presents the UV–vis spectroscopic investigation of the Dex-PL-A crosslinker. It reveals an absorption maximum at 260 nm accompanied by the anticipated additional absorption maximum at 350 nm. Thus, the crosslinker exhibits a high absorption in the targeted photolysis wavelength region of $\lambda > 315$ nm.

Photolysis of the Cleavable Crosslinker in Solution

To investigate the photolytic performance of the newly synthesized photocleavable crosslinker, time dependent UV–vis measurements of Dex-PL-A in aqueous solution were performed. The respective spectra are shown in Figure 2.

Irradiation with UV light of the wavelength of $\lambda = 365$ nm resulted in a red shift of the absorption maximum at 350 nm and the evolution of two new absorption bands at 235 nm and 270 nm. In addition, absorbance at 305 nm decreased upon irradiation as shown in magnification in the inset of Figure 2(a). Along with these light-induced changes in the spectra, the occurrence of well-defined isosbestic points over the complete irradiation time scale points toward a successful cleavage of the chromophore, which is supposed to be a first-order reaction. As shown in Figure 2(b), the rate of decrease of the absorbance at 305 nm during irradiation followed an exponential decay to a constant level at 176 s. Kinetic analysis was performed by setting the value of the final absorbance at 245 s as zero. The resulting kinetic plot of $-\ln [CL]_t/[CL]_0$ versus time shows excellent linearity, indicating the expected first-order kinetic with respect to the chromophore concentration. The observed well-defined photolytic cleavage in short time scales under mild irradiation conditions in combination with the polymerizable acrylate functionalities and the enzymatically degradable dextran backbone renders these newly synthesized molecules highly interesting as double stimuli-sensitive crosslinkers for the formation of degradable hydrogels from aqueous solutions.

Preparation and Characterization of Hybrid p(AAm-*co*-Dex-PL-A) Gel Nanoparticles by Inverse Miniemulsion Copolymerization

Nanogel particle formation can be achieved by different approaches including precipitation (co)polymerization from aqueous solutions,[1,2] crosslinking of preformed polymers in (mini)emulsions, or copolymerisation of crosslinkers and monomers in inverse miniemulsion.[33] Because degradable

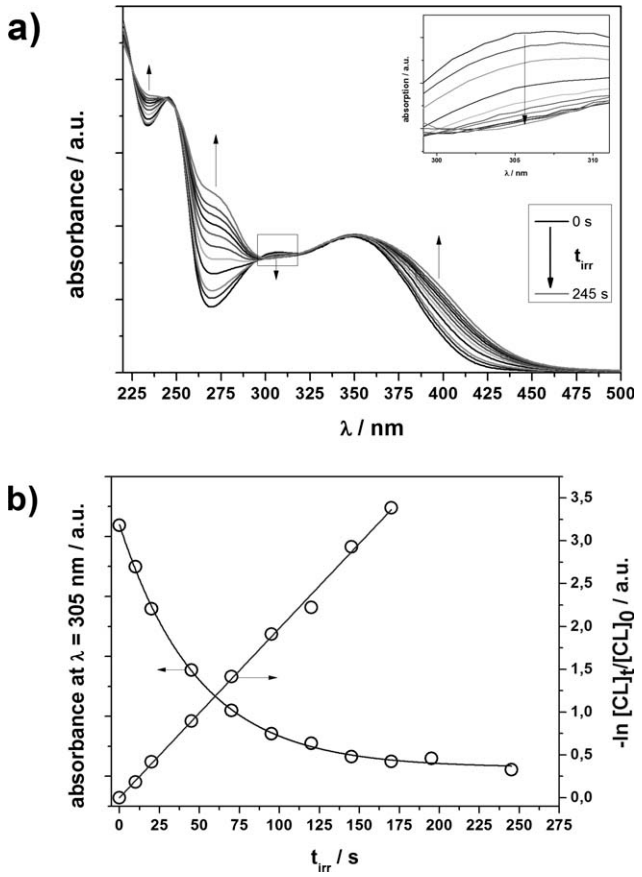

FIGURE 2 Irradiation of Dex-PL-A in aqueous solution: (a) time dependent UV–vis spectra; (b) time-dependent absorbance at $\lambda = 305$ nm including the exponential fit and kinetic plot of $-\ln [CL]_t/[CL]_0$ versus time including the linear fit.

nanogels are great potential systems for the embedding and release of active functional compounds upon the appliance of one or more orthogonal triggers, nanogel preparation based on inverse miniemulsion bears a big advantage compared with other methods. In this process, the addition of an osmotic agent (an ultrahydrophilic compound) such as sodium chloride to the dispersed phase prevents diffusion between the droplets by creating an osmotic pressure which counteracts the Laplace pressure. Therefore, stable droplets of the same composition are obtained and can be classified as "nanoreactors."[34] As a result, the composition of the latex particles after polymerization resembles the composition of the monomer phase, thus enabling the equal distribution of all different functionalities in each particle.[35] The potential embedding of functional compounds is therefore highly facilitated. Moreover, when compared with precipitation polymerization based approaches, the equal distribution of crosslinkers in the gel particles enables a better comparability of the resulting gel properties such as the DGS among the different nanogels prepared.

To prepare hybrid p(AAm-*co*-Dex-PL-A) nanogel particles, AAm and Dex-PL-A were dissolved in an aqueous sodium chloride solution and copolymerized in inverse miniemulsion

TABLE 1 Synthetic Details for the Inverse Miniemulsion Copolymerizations of Hybrid Nanogels

Classific.	Sample	AAm (m/g)	Dex-PL-A (m/g)	m(Dex-PL-A)/ [m(Dex-PL-A) + m(AAm)] (%)	Solvent of Dispersed Phase Type (m/g)	Initiator Type
Set A	HNG-1A	0.950	0.050	5.0	0.5 M NaCl (1.00)	V-59
	HNG-2A	0.825	0.175	17.5	0.5 M NaCl (1.00)	V-59
	HNG-3A	0.700	0.300	30	0.5 M NaCl (1.00)	V-59
Set B	HNG-1B	0.950	0.050	5.0	0.5 M NaCl (1.00)	V-70
	HNG-2B	0.825	0.175	17.5	0.5 M NaCl (1.00)	V-70
	HNG-3B	0.700	0.300	30	0.5 M NaCl (1.00)	V-70
	HNG-4B	0.400	0.600	60	0.5 M NaCl (1.00)	V-70

by free radical polymerization. Table 1 lists the composition of the different nanogels in combination with the type of initiator (see "Experimental" section). Two sets of experiments were performed to demonstrate the versatility of this preparation method. Although hybrid nanogels HNG-1A–HNG-3A of set A were polymerized at 70 °C using V-59 as radical initiator, V-70 was used for the preparation of set B (HNG-1B to HNG-4B) by initiating the polymerization at a much lower temperature of 37 °C. With regard to a potential embedding of active compounds, a lower polymerization temperature holds promise for the embedding of sensitive compounds at mild conditions.

Another important factor to be considered during nanogel preparation is the crosslinking density of the resulting network. Especially in the context of potential carrier applications, the prepared nanogels should exhibit a low initial DGS to prevent diffusion of embedded compounds from the network. Even though this parameter can be adjusted by increasing the Dex-PL-A/AAm ratio (i.e., the amount of crosslinking points on the dextrane), a balance between a low initial DGS and a good enzymatic degradability is of high importance. Incorporation of too many crosslinking points is known to hinder enzymatic degradation of the dextran chains due to a reduced accessibility caused by too small mesh sizes of the gel.[15] Hence, in every set of nanogels, the amount of Dex-PL-A crosslinker was varied with the intention to investigate the influence of the Dex-PL-A/AAm ratio on the properties of the resulting microgels. For polymerizations at 70 °C HNG-1A contained 5 wt %, HNG-2A 17.5 wt %, and HNG-3A 30 wt % of Dex-PL-A, respectively. Analogously, the gel particles HNG-1B–HNG-4B of the second set contained 5.0, 17.5, 30, and 60 wt % of Dex-PL-A. All polymerizations were carried out overnight, and the resulting dispersions were washed repeatedly with cyclohexane to remove excess surfactant. The resulting stable dispersions of hybrid nanogels in cyclohexane were investigated with regard to the hydrodynamic diameter by dynamic light scattering (DLS) measurements and the particle morphologies and sizes were determined by scanning electron microscopy (SEM). Figure 3 shows representative SEM pictures of HNG-3A in comparison with HNG-3B as well as the respective

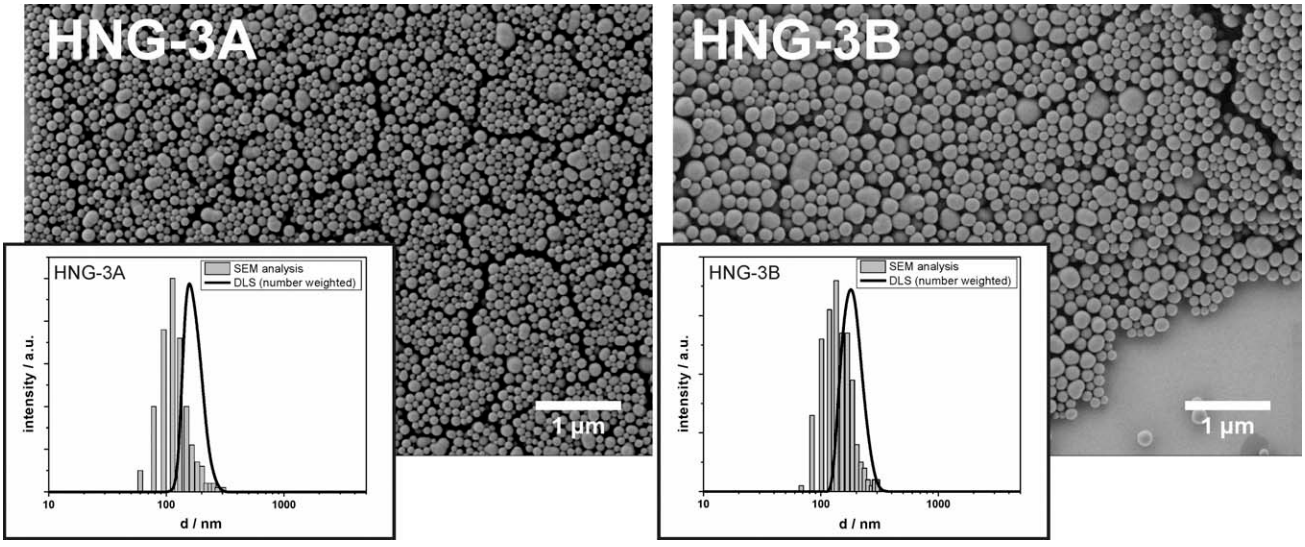

FIGURE 3 Representative SEM pictures HNG-3A and HNG-3B nanogels dropcast from cyclohexane dispersion and size distributions obtained from DLS measurements (number weighted) in comparison with diameters obtained from SEM analysis.

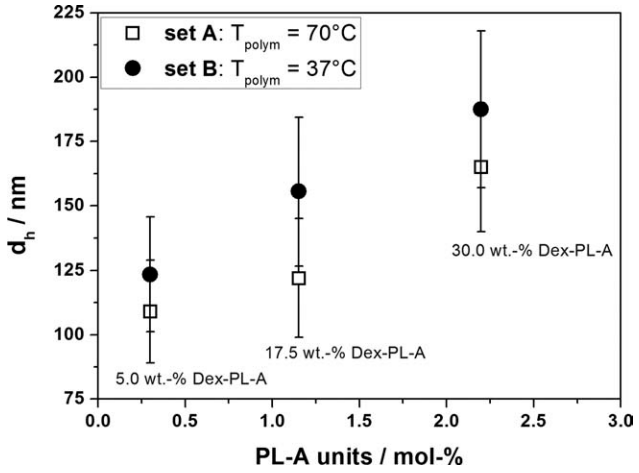

FIGURE 4 Hydrodynamic diameters of hybrid nanogels obtained from DLS measurements in cyclohexane dispersion after washing.

number weighted size distributions obtained from DLS and SEM analysis. Figure 4 shows the hydrodynamic diameters of the particles in cyclohexane in dependency on the amount of acrylate groups available for crosslinking.

As can be seen from SEM photographs, inverse miniemulsion copolymerizations yielded well-defined spherical hybrid gel particles with nanoscale dimensions. From the hydrodynamic particle diameters shown in Figure 4, it becomes obvious that for an increasing amount of polymerizable acrylate units—realized by increasing the Dex-PL-A/AAm ratio—the particle size also increases. This effect is assumed to be based on an increased viscosity of the monomer phase for higher contents of functionalized dextrans. Because droplet formation in the miniemulsion procedure derives from a fission and fusion process upon appliance of high shear forces by ultrasonication, a higher viscosity of the dispersed phase hinders the disrupture of bigger droplets of the preemulsion. When comparing the hydrodynamic diameters obtained from DLS measurements to the diameters from SEM photographs (see Fig. 3), it becomes apparent that the values from light scattering in cyclohexane dispersion are larger than those obtained from the dried particles. As water was added as a solvent for the monomer phase, it is still present in the formed gel particles after polymerization. When compared with the collapsed dried particles observed by SEM, nanogels in cyclohexane dispersion consist of swollen networks resulting in increased particle diameters.

At very high Dex-PL-A contents (60 wt %), increasing polydispersity and ill-defined morphologies were observed (data not shown). In this case, the high amount of the functionalized dextran influences the stability of the droplets due to the surface active character of the amphiphilic Dex-PL-A. Because attempts to form nanogels from pure Dex-PL-A did not yield stable miniemulsions, the presence of a second comonomer is a crucial requirement for the formation of enzymatically and light degradable gel particles by inverse miniemulsion polymerization.

The transfer of the gel particles to the aqueous phase was easily achieved by immersing the freeze dried particles over night in water. Repeated washing of the swollen nanogels with deionized water removed the soluble fraction of the crosslinking polymerization reaction. Resulting dispersions of the nanogels in water were stable without any additional surfactant due to sterical stabilization of dangling chains of the swollen outer particle layer. The washing phases and the aqueous particle dispersions were freeze dried separately and gravimetric analysis yielded the respective sol/gel contents. The sol fraction consisted of all unreacted monomers and noncrosslinked polymers and oligomers. Because a lower sol content reflects a higher crosslinking efficiency, its determination enables the relative evaluation of the performance of the crosslinking copolymerization. As mentioned above, the swelling ratio or the DGS is another important property of the nanogels. It is determined by calculating the volume ratio of swollen nanogels in water to nonswollen dried nanogels via DGS $= V_{\text{swollen}}/V_{\text{nonswollen}}$. The volume of the swollen particles was determined by DLS measurements of the aqueous dispersions, whereas the volume of the nonswollen particles was calculated from the diameters obtained from SEM photographs of the dried gel particles from cyclohexane dispersions. Similar to the sol content, this parameter is an indication for the efficiency of the crosslinking reaction, because a lower initial DGS is based on a smaller mesh size of the network caused by the incorporation of more crosslinking points. Figure 5(a) shows the values for the sol contents and initial DGSs obtained by gravimetric analysis and DLS measurements. Although determination of either parameter does not permit to draw quantitative conclusions regarding the crosslinking density or the inner morphology of the nanogels, it nevertheless allows the expedient relative comparison of the gel properties among the different samples.

Figure 5(a) shows the dependency of Dex-PL-A/AAm feed ratio to DGS values and sol contents. As expected, increasing the feed ratio of Dex-PL-A/AAm [i.e., the theoretical amount of polymerizable photolabile linker acrylate (PL-A) groups] for a fixed polymerization temperature, reduces both the sol content and the initial DGS. Both parameters indicate a higher copolymerization efficiency.

When comparing the properties of the gel particles polymerized at 70 °C to those of the nanogels polymerized at 37 °C it becomes obvious that for similar feed ratios of Dex-PL-A/AAm, a lower polymerization temperature resulted in increased sol contents and lower degrees of swelling. This effect can be assigned to comparably lower conversions of the polymerization reactions. The decreased reaction temperature hinders diffusion of monomers and increases the probability of termination reactions. Because ^{1}H NMR analysis of the sol content (data not shown) revealed only negligible amounts of Dex-PL-A, quantitative incorporation of the crosslinking molecules is assumed. Based on the ensuing presumption that the sol content consisted only of unreacted AAm monomers and oligomers, the effective Dex-PL-A/AAm ratios were calculated. Figure 5(b) shows the calculated

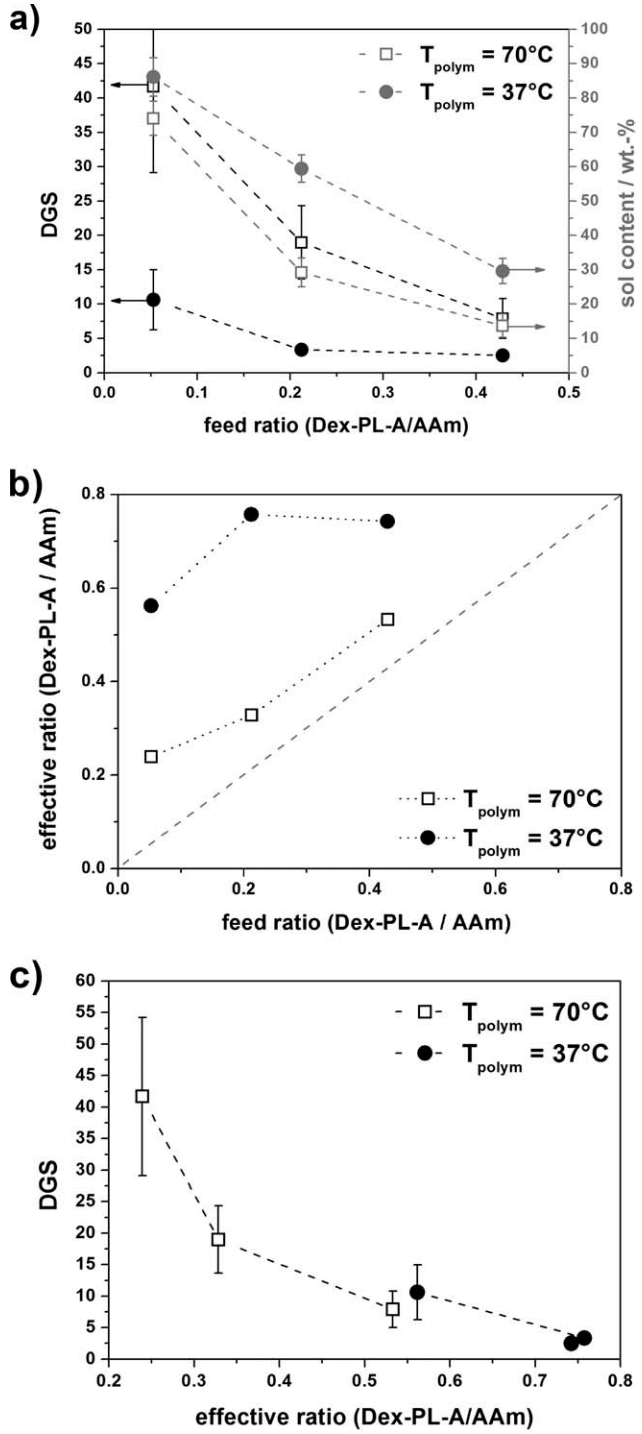

FIGURE 5 Characterization of the gel properties of the hybrid p(AAm-*co*-Dex-PL-A) nanogels: (a) DGS and sol content values in dependency on the feed ratio of Dex-PL-A/AAm. Empty squares: nanogels of set A polymerized at 70 °C, filled dots: nanogels of set B polymerized at 37 °C; (b) effective ratio of Dex-PL-A/AAm in comparison with the respective feed ratio, the diagonal represents the ideal case of quantitative incorporation of both compounds and is a guide for the eye; (c) DGS values in dependency on the effective ratio of Dex-PL-A/AAm; empty squares: nanogels of set A polymerized at 70 °C, filled dots: nanogels of set B polymerized at 37 °C.

values plotted against the theoretical values; that is, the feed ratios of Dex-PL-A/AAm. It is seen that for the same Dex-PL-A/AAm feed ratio, higher sol contents for the nanogels polymerized at 37 °C correlate with increased effective Dex-PL-A/AAm ratios compared with the samples polymerized at 70 °C.

Plotting the DGS values of the two sets of nanogels against the effective Dex-PL-A/AAm ratio shows the anticipated trend of decreasing degrees of swelling with increasing amounts of actually incorporated crosslinking molecules [Fig. 5(c)]. The favored incorporation of functionalized dextran for the lower polymerization temperature (37 °C) is therefore expected to yield nanogels consisting of networks with smaller mesh sizes. Additionally, with increasing feed ratios of Dex-PL-A/AAm, a decreasing deviation of the effective ratios from the theoretical values is observed for both polymerization temperatures. This confirms a higher crosslinking efficiency if more Dex-PL-A crosslinking molecules are available.

The systematic variation of the Dex-PL-A/AAm ratio [Fig. 5(a)] revealed HNG-3B nanogels as the most promising candidates for potential release applications for three reasons: (i) The observed relatively low sol content of 29.6 wt % mainly consisted of AAm monomers and oligomers, therefore pointing toward a successful crosslinking copolymerization with an almost quantitative incorporation of Dex-PL-A crosslinking molecules. (ii) The low initial DGS of 2.5 is potentially effective for the embedding of functional compounds. (iii) The substantially low polymerization temperature of 37 °C renders these synthetic parameters highly effective.

Photolytic and Enzymatic Degradation

Because hybrid p(AAm-*co*-Dex-PL-A) nanogels HNG-3B exhibited the desired gel properties, their degradation behavior upon irradiation and treatment with dextranase was investigated to demonstrate their potential for release applications. Degradation experiments were conducted in aqueous dispersions with a solid content of 0.0625% consisting of purified nanogels.

Partial cleavage of crosslinking points by either photolytic disrupture of the connecting bonds between polyacrylamide chains and dextrans or the enzymatic decomposition of the latter should result in a loosened network structure with increased mesh sizes, thus yielding gel particles of an increased DGS. Further exposure to the respective stimuli is expected to form completely disintegrated networks consisting of freely soluble polymer chains and dextran oligomers. Generally, DLS measurements can be applied to determine increased particle sizes caused by the higher DGS but are limited to the partial degradation regime. To investigate the complete degradation behavior, turbidity measurements can be used as they are capable of visualizing the complete time dependent photolytic and enzymatic particle disintegration as well.

As shown in a previous publication,[25] an increase of the DGS corresponds to a loosening of the network structure due to the cleavage of crosslinking points and causes a decreased contrast in the refractive indices between solvent and particle.[36,37] As a

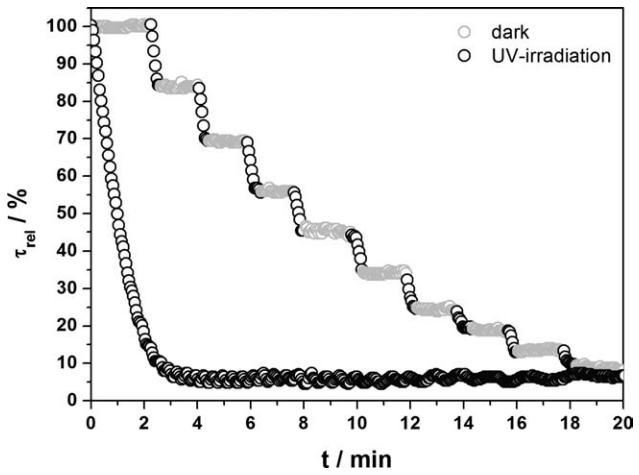

FIGURE 6 Turbidity measurements for the irradiation of an aqueous HNG-3B nanogel dispersion (0.0625% w/v) with UV light ($\lambda = 365$ nm, $I = 30$ mW/cm^2).

result, the scattering intensity decreases, leading to optically more transparent dispersions. Quantification of this phenomenon can be achieved by calculating the turbidity $\tau(t)$ as the intensity ratio of transmitted light of the sample I_t to transmitted light of pure water I_0 as $\tau(t) = -\ln I_t/I_0$. The respective relative values were then obtained as the ratio of the time dependent turbidity after exposure to the respective stimulus to the starting values $\tau(t = 0)$ as $\tau_{rel} = \tau(t)/\tau(t = 0)\cdot 100$.

First, the photolytic cleavage of the *o*-nitrobenzylester groups connecting polyacrylamide chains to dextrans was investigated. Two different experiments were performed: constant and stepwise irradiation of the sample with UV light. Figure 6 shows the resulting plots of turbidity versus time.

The plot clearly shows a profound decrease of the relative turbidity down to a constant level of almost 0% after only ~3 min of continuous irradiation, thus indicating complete particle degradation in a short time scale under mild conditions. This observation was confirmed since attempts to perform DLS measurements on the resulting clear solution did not yield any results regarding particle sizes. The stepwise irradiation was performed by repeated cycles of irradiating the sample for each time 15 s and then keeping the sample in the dark for 2 min. Turbidity was monitored during the whole process and was found to decrease only during the appliance of light. Because turbidity—and therefore the degradation—is not altered in the dark, the photolytic decomposition of the nanogels can be stopped at any desired degree, thus proving a highly controlled photodegradation profile.

The observed stepwise degradation allowed the detailed investigation of the photolytic decomposition at fixed time points of irradiation. Samples were withdrawn after every irradiation step and analyzed. The chromophore cleavage was investigted by UV–vis spectroscopy and the particle size assessed by means of DLS measurements. Figure 7(a) shows the respective normalized irradiation time dependent UV–vis spectra, whereas Figure 7(b) depicts the respective hydrodynamic diameters of the irradiated nanogels in comparison with the relative transmittance of the dispersion.

Irradiation time dependent UV–vis measurements clearly show the successful cleavage of the photolabile *o*-nitrobenzyl ester linkers. When compared with the photolysis of pure Dex-PL-A crosslinking molecules in solution, the spectra of the respective nanogels are influenced by scattering of the dispersion. As seen by turbidity measurements, the scattering intensity decreases upon irradiation and no isosbestic points were observed in the raw UV–vis spectra (data not shown). Nevertheless, the change in absorbance at 270 nm relative to the absorbance at 300 nm clearly points to a successful photoreaction. Because UV–vis spectroscopy of the irradiation of pure Dex-PL-A exhibited an isosbestic point at $\lambda = 330$ nm, normalizing the spectra of the nanogels to the final absorbance after 165 s of irradiation at this wavelength yielded the same well-defined isosbestic points as well. Hence, it was concluded that the photoreaction is not influenced by the gel matrix.

DLS measurements of the irradiated samples clearly show the increase of particle sizes in dependency on the irradiation time. As expected, the light-induced cleavage of covalent

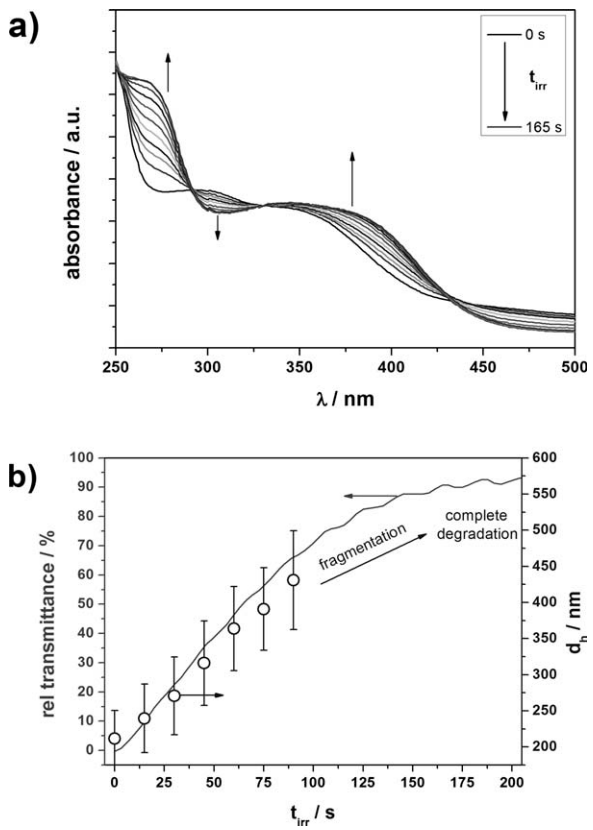

FIGURE 7 (a) Irradiation time dependent UV–vis spectra of HNG-3B nanogels (normalized to $\lambda = 330$ nm at $t_{irr} = 165$ s); (b) irradiation time-dependent hydrodynamic diameters of HNG-3B nanogels in comparison to the relative transmittance of the respective aqueous dispersion.

bonds between polyacrylamide and dextran chains results at first in highly swollen nanogels characterized by a loosened network structure and later in completely soluble polymer chains. Although DLS measurements of irradiated nanogels up to irradiation times of 90 s yielded well-defined monomodal size distributions, the determination of hydrodynamic diameters for longer irradiation times exhibited multimodal distributions due to fragmentation of the gels. For even longer irradiation times, no results were obtained due to a too low scattering intensity. As speculated before, the results confirm that DLS characterization is indeed only possible in the partial degradation regime. In contrast, the performed turbidity measurements clearly are highly advantageous to investigate the full degradation profile. The correlation between increasing particle sizes and increasing transparency (i.e., decreasing scattering intensity) is confirmed by the plot in Figure 7(b).

In summary, the experiments demonstrate that the complete photolytic disintegration of the hybrid p(AAm-*co*-Dex-PL-A) network structure upon cleavage of the covalent bonds between PAAm and dextran can be achieved fast and quantitatively under mild irradiation conditions. Moreover, the well-defined photoreaction even allows only partial degradation of crosslinking points and therefore nanogels of a desired specific DGS can be obtained by adjusting the irradiation time accordingly.

To demonstrate the double stimuli-responsive character of the hybrid nanogels, further degradation experiments were conducted to investigate the enzymatic dextran chain cleavage upon the addition of dextranase. In principal, the degradation of the dextran backbone in the Dex-PL-A crosslinkers should lead to a disintegration of the polymeric network and result in either fully degraded gels or particles exhibiting an increased DGS (for incomplete dextran chain cleavage). Investigations were carried out on aqueous dispersions of the purified HNG-3B gel particles (0.0625% w/v) at 37 °C, and turbidity of the sample was monitored after the addition of a dextranase solution. The resulting curve is shown in Figure 8(a).

The initial turbidity decreases as a function of incubation time until it reached a constant value of 50% after circa 5 h. Even though no complete particle degradation—corresponding to a relative turbidity of ~0%—was achieved, the drop in turbidity can be assigned to an increased DGS of the hydrogel particles. The corresponding increased pore size of the network results from partial cleavage of the dextran backbones responsible for the crosslinking of gel. DLS measurements were conducted to confirm this assumption and the resulting size distributions before and after enzymatic treatment are shown in Figure 8(b). As expected, the particle size increased from an initial diameter of 212 nm to 344 nm, thus corresponding to a change in DGS from the low initial value of 1.4 to the final value of 6.2. When comparing the measured hydrodynamic diameter of 344 nm after enzymatic treatment—corresponding to a turbidity of 50%—to the measured diameter of 364 nm after 60 s of UV irradiation—corresponding to a similar turbidity of ~50%—

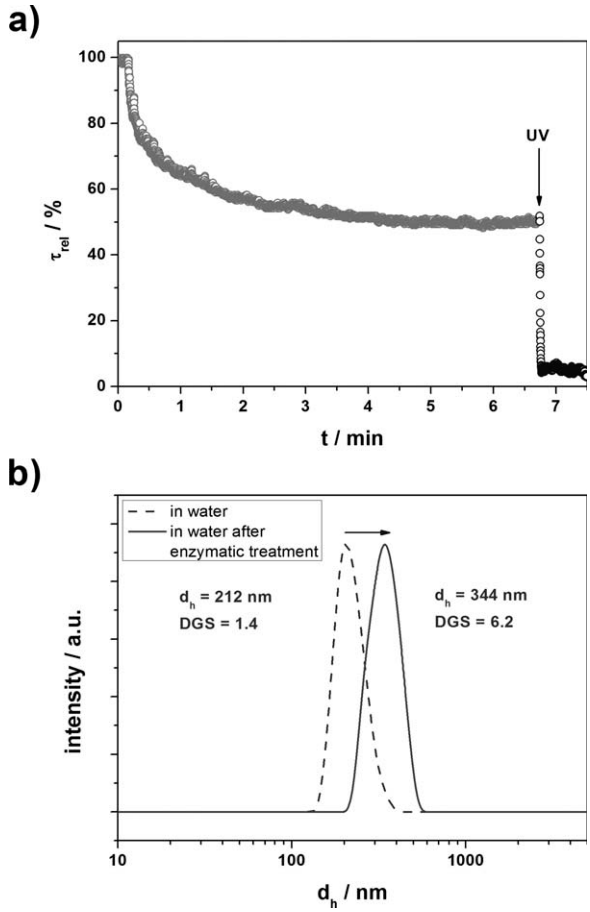

FIGURE 8 Enzymatic and subsequent photolytic degradation of HNG-3B nanogels: (a) turbidity curve; (b) particle size distributions before and after enzymatic treatment measured by DLS.

the similar particle sizes once again demonstrate the good correlation between turbidity and degree of degradation (i.e., DGS). Moreover, these results point towards a comparable degradation mechanism including the increase in mesh sizes by cleavage of crosslinking points.

Because any treatment with the enzyme for longer times did not yield a further decay of the turbidity—that is, breakage of dextran chains—the final value represents the crucial limit for enzymatic particle degradation. This observed limitation can in general be based on various effects.

On one hand Franssen et al. proposed that the enzymatic degradation of crosslinked dextran methacrylates is influenced by the accessibility of the dextran chains for dextranase.[15] Because of the presence of interpenetrating networks and the fact that the dextran chains are severely strained this factor is reduced. In addition, the overall amount of crosslinking points in the network can also play a crucial role since the diffusion of the enzyme through the hydrogel matrix is decreased as a result of a screening effect.[15] Imagining a high density of crosslinking points (i.e., small mesh sizes), this would give access to the enzymatic degradation of the outer sphere due to an enhanced accessibility of the

surface. The comparably large size of the dextranase enzyme (44 kDa) may hinder complete particle degradation due to inaccessible inner parts of the particle core caused by small mesh sizes.

On the other hand, the interaction between the functionalized dextran chains and the active sites of the enzyme was found to depend on the character of the substitution of the polysaccharide.[14,15] Although Franssen et al. demonstrated that dextranase is capable of hydrolyzing a bond between a substituted and an unsubstituted glucopyranose residue of dextran methacrylates in solution, a cleavage of bonds between two substituted glucopyranose residues cannot be achieved by the enzyme. Regarding the case of Dex-PL-A crosslinkers, the functionalization of the dextran chains with PL-A moieties is assumed to yield statistically distributed substitution of glucopyranose residues meaning that functionalization of two neighboring groups in the dextran chain occurs as well. As in the resulting hydrogel matrix pAAm chains are also connected by this specific structural unit, the hindered enzymatic cleavage of the latter results in incomplete network degradation.

Finally, the overall DS can play an important role as well. Dextran methacrylates with low DS values (and resulting hydrogels) can easily be cleaved by dextranase yielding isomaltose and methacrylated isomaltotriose as the main degradation products.[14] Long unsubstituted chain segments of dextran (i.e., 18 or more unsubstituted glucopyranose units) are assumed to have enough conformational freedom to fold correctly in the binding site of dextranase, thus enabling multiple scissions by the enzyme with a rate similar to that of native dextran. For increasing degrees of substitution, the corresponding shorter unsubstituted chain segments are restricted in their conformational freedom by neighboring substituted glucopyranose residues. Even though these chain segments can still bind to the binding site of the enzyme, the affinity and corresponding degradation rate is decreased. As mentioned before, the DS of 0.17 of Dex-PL-A is related to free chain segments of ~6 unsubstituted glucopyranose units. As this value was found to be the lower critical value for successful hydrolysis of crosslinked dextran methacrylates, the observed partial degradation can be also assigned to a reduced affinity of Dex-PL-A to the binding sites of dextranase.

Summarizing the statements made above, incomplete microgel degradation upon treatment with dextranase is assumed to be based on: (i) the reduced accessibility of the dextran chains in the interpenetrating p(AAm-*co*-Dex-PL-A) network for the enzyme; (ii) hindered cleavage of two neighboring substituted glucopyranose residues; and (iii) decreased affinity of the Dex-PL-A to the binding site of the enzyme due to the relatively high DS. Nevertheless, the observed sixfold increase in particle volume after treatment with dextranase holds great potential for the release of functional compounds from the network triggered by increasing mesh sizes.

Having demonstrated partial enzymatic degradation, the question arises whether complete particle disintegration can be subsequently achieved by irradiation of the swollen nanogels. As shown in Figure 8(a), this pathway could indeed be used to realize a two-step degradation profile. After the hybrid nanogel particles reached the maximal DGS upon treatment with dextranase, irradiation of the swollen gel particles led to complete particle degradation as demonstrated by a measured turbidity of ~0%. An additional advantage is the comparably much faster response to the trigger. Because enzymatic treatment can induce a continuous but slow degradation profile (~6 h), the photolytic degradation can be achieved in less than 2 min.

To verify the results presented above, SEM pictures of HNG-3B nanogel dispersions at different points of the two-step degradation were taken and are shown in Figure 9.

The initial nondegraded particles can be identified as flattened spheres on the silica wafer [Fig. 9(a)]. Even though drying of the particles from the swollen state resulted in film formation and flattened structures, the retention of the spherical morphology clearly hints again to the successful crosslinking of PAAm by Dex-PL-A. After irradiation with UV light, no spherical structures were observed by SEM but a polymeric film [Fig. 9(b)], thus indicating complete particle degradation. As shown in Figure 9(c), after the enzymatic treatment particular structures were still observed but an increasing film formation/flattening is visible, caused by the highly swollen state of the nanogels before drop casting. Finally, in Figure 9(d), no particular structures were detected and the observed polymer film results from the completely degraded nanogels upon UV irradiation subsequent to the enzymatic treatment.

Summarizing the degradation behavior of the p(AAm-*co*-Dex-PL-A) hybrid nanogels three different degradation profiles were realized. At first, the exclusive photolytic cleavage of the photolabile linkers between dextran and PAAm chains was successfully used to fully degrade the nanogels upon continuous irradiation in a short time span. Partial degradation of crosslinking points and therefore nanogels of a desired specific DGS were obtained by adjusting the irradiation time accordingly. Second, partial enzymatic cleavage of the dextran backbones of the Dex-PL-A crosslinking molecules resulted in an increase of the DGS of the nanogels up to a constant value. Third, the subsequent irradiation of those swollen hydrogel particles could be used to fully degrade the network structure. Hence, by combining the two orthogonal stimuli, a two-step degradation profile was realized rendering such hybrid nanogels highly versatile materials for potential release applications.

EXPERIMENTAL

Materials

All chemicals were commercially available and used without further purification unless otherwise stated. AAm was obtained by Fluka chemicals and Lubrizol U was kindly provided by Lubrizol, France. All other chemicals and solvents were obtained by Sigma Aldrich.

Instrumentation

^{1}H (300 MHz) spectra were measured using a Bruker spectrometer. Particle size distributions were determined by DLS

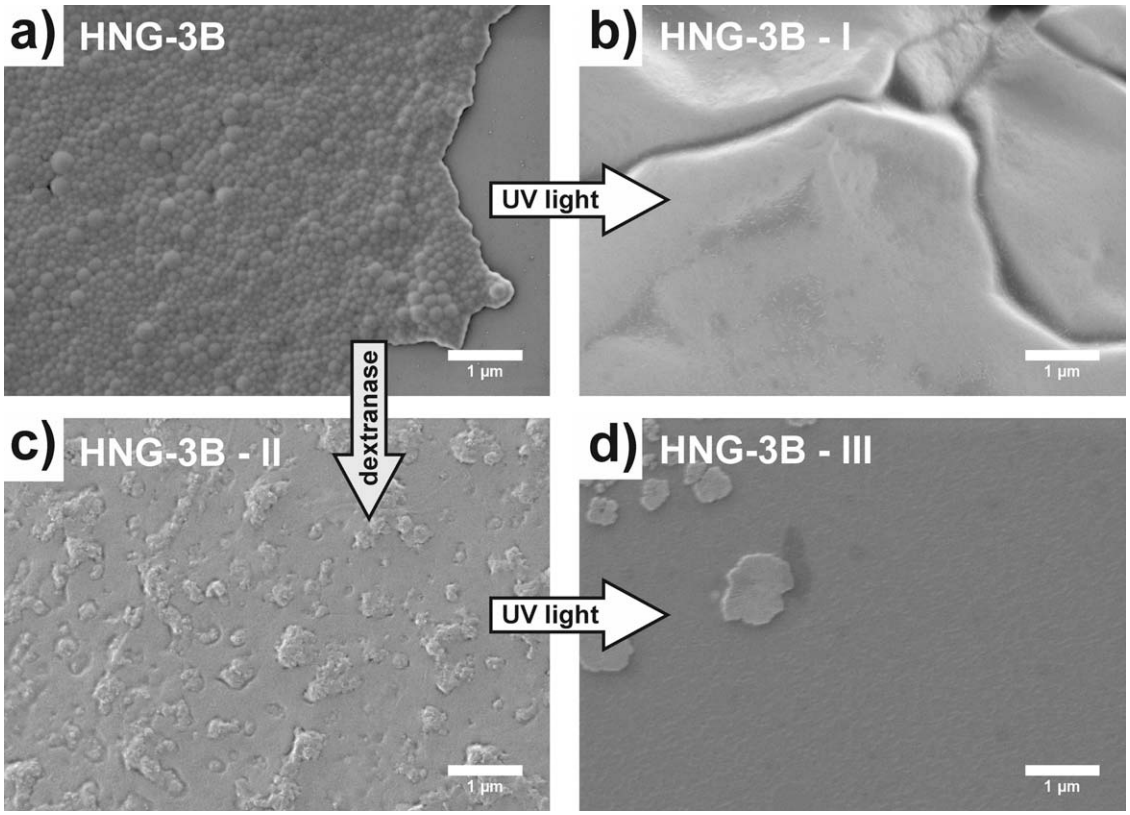

FIGURE 9 SEM investigations on the stimuli-induced degradation behavior of HNG-3B: (a) swollen microgels in water; (b) completely degraded microgels after UV irradiation; (c) highly swollen microgels after treatment with dextranase; (d) completely degraded microgels after first enzymatic treatment and subsequent irradiation with UV light.

using a NICOMP zetasizer measuring at a fixed scattering angle of 90°. The measurements were carried out at 25 °C on diluted dispersions in the respective solvents. Turbidity measurements were performed in transmission using a He-Ne Laser and a photo diode. A Gemini 1530 (Carl Zeiss AG, Oberkochem, Germany) with an InLens detector was used to take SEM. The samples were prepared by drop-casting of diluted dispersions on a silicon wafer. UV–vis spectra of crosslinkers in solution were determined by using a Perkin Elmer Lambda 25 UV/VIS spectrometer. The respective irradiation time dependent UV–vis spectra of the nanogels were measured by using a TECAN plate reader and a Hellman 96-well quartz plate.

Synthesis of Dextran-Photolabile Linker-Acrylate

Dex-PL-A was obtained by first synthesizing the carboxylic acid functionalized photolabile linker molecule containing the acrylate moiety and subsequent coupling with dextran. Scheme 1 shows the synthetic pathway and the reaction conditions.

4-(4-(1-Hydroxyethyl)-2-methoxy-5-nitrophenoxy) butanoic acid (HEMNPBA) (5)

As described in a previous publication,[25] the product was prepared based on the synthetic protocols by Holmes.[27,38] Briefly, acetovanillone was reacted with methyl 4-bromobutyrate in the presence of potassium carbonate to form the corresponding keto ester. After removing the inorganic salts by extraction with ethyl actetate, subsequent nitration of the crude product was achieved by the reaction with acetic anhydride and nitric acid (1:2 v/v). In the next step, the reduction of the keto group with excess borohydride was conducted and directly followed by inducing the ester cleavage by addition of NaOH in water. Purification by recrystallization from ethyl acetate/hexane afforded HEMNPBA (5) in 89% yield as a pale yellow solid.

^{1}H NMR ($CDCl_3$): δ = 7.41 (s, 1H), 7.24 (s, 1H), 5.37 (q, J = 6.2 Hz, 1H), 3.97 (t, J = 6.4 Hz, 2H), 3.82 (s, 3H), 2.37 (t, J = 7.2 Hz, 2H), 2.00 (p, J = 6.8 Hz, 3H), 1.35 (d, J = 6.3 Hz, 1H). ^{13}C NMR ($CDCl_3$): δ = 174.92, 154.05, 146.56, 139.12, 138.33, 108.97, 108.89, 68.24, 64.95, 56.23, 30.18, 24.84, 24.18. MS (FD) m/z 299.2 (M^+).

4-(4-(1-(Acryloyloxy)ethyl)-2-methoxy-5-nitrophenoxy)-butanoic acid (AEMNPBA) (6)

HEMNPBA (1.000 g, 3.34 mmol) was dissolved under argon in anhydrous dichloromethane (40 mL). Triethylamine (1.014 g, 10.00 mmol) was added and the solution was cooled to 0 °C. Acryloyl chloride (0.756 g, 8.35 mmol) was dissolved in 10 mL of anhydrous dichloromethane and added dropwise to the reaction vessel. The mixture was stirred over night and allowed to warm up to room temperature. Afterward, the solution was washed in every case thrice with sodium carbonate solution, diluted hydrochloric acid, and deionized water. The organic solvent was evaporated

under reduced pressure and the resulting solid was stirred in aceton/water over night. Insoluble contents were removed by filtration, and the remaining phase was extracted thrice with dichloromethane. The combined organic layers were washed with diluted hydrochloric acid and deionized water, dried over $MgSO_4$, and the solvent was removed. The remaining yellow solid was purified by column chromatography over silica using $CHCl_3$/MeOH 10:1 v/v as eluent and pure AEMNPBA (0.771 g, 2.18 mmol) was obtained in 65% yield as yellow solid.

^{1}H NMR ($CDCl_3$): $\delta = 7.59$ (s, 1H), 7.00 (s, 1H), 6.53 (q, 1H, $J = 6.4$ Hz), 6.43 (dd, 1H, $J = 1.5$ Hz, $J = 17.3$ Hz), 6.15 (dd, 1H, $J = 10.4$ Hz, $J = 17.3$ Hz), 5.87 (dd, 1H, $J = 1.5$ Hz, $J = 10.4$ Hz), 4.12 (t, 2H, $J = 6.2$ Hz), 3.92 (s, 3H), 2.61 (t, 2H, $J = 7.1$ Hz), 2.18 (m, 2H), 1.65 (d, 1H, $J = 6.4$Hz). ^{13}C NMR ($CDCl_3$): $\delta = 178.44$, 164.93, 154.04, 147.15, 139.79, 133.34, 131.39, 128.23, 109.10, 108.14, 68.63, 68.04, 56.28, 30.22, 23.97, 22.01.

Dextran-Photolabile Linker-Acrylate (8)

In the first step, oxalyl chloride (0.333 g, 2.62 mmol) in 5 mL of anhydrous dichloromethane was added dropwise to an ice cooled solution of AEMNPBA (0.771 g, 2.18 mmol) in 30 mL of anhydrous dichloromethane under argon. Few drops of DMF were added, and the mixture was stirred at room temperature for 2.5 h. The solvent was removed under reduced pressure and the flask was vented with argon. The resulting oil was dissolved in 5 mL of anhydrous DMF and added dropwise to a solution of dextran (6000 g/mol, 1.596 g, 0.226 mmol, 9.044 mmol glucopyranosyl groups), LiCl (4.0 g), and NEt_3 (0.572 g, 3.39 mmol) in 50 mL of anhydrous DMF. The reaction mixture was stirred at room temperature over night and then heated to 60 °C for 1 h. After cooling the solution to room temperature, the modified dextran was obtained by precipitation in isopropanol. The crude product was dissolved in water, precipitated again in isopropanol. This purification procedure was repeated for a total of two times and the functionalized dextran was obtained in 58% yield as slightly yellow colored powder from freeze drying of the aqueous solution. The DS was obtained from ^{1}H NMR spectroscopy by calculating the peak area ratio of the 6 (olefinic, aromatic, and tertiary benzylic) protons assigned to the multiplets from 7.70 to 5.60 ppm relative to the anomeric protons of dextran assigned to the multiplet at 5.25–4.75 ppm by using the formula:

$$\mathrm{DS(Dex-PL-A)} = \frac{A[6\mathrm{H(PL-A)@7.70-5.60\ ppm}]/6}{A[1\mathrm{H(anomeric)@5.25-4.75\ ppm}]}$$

A DS of 0.17 was determined meaning that in a dextran chain of 34 glucopyranosyl groups every sixth group is functionalized with the photolabile linker-acrylate.

Synthesis of Hybrid Nanogels by Inverse Miniemulsion Copolymerization

The dispersed phase was prepared by dissolving various amounts of AAm and Dex-PL-A in a 0.5 M NaCl solution. Afterward, the mixture was added to the continuous phase consisting of a solution of the nonionic surfactant Lubrizol U (100 mg) in 10 g of cyclohexane. The miniemulsion was formed by first stirring the mixture at 1750 rpm for 1.5 h and then homogenizing the obtained pre-emulsion by ultrasonication for 2 min at 90% intensity (Branson sonifier W450 Digital, 0.5" tip) at 0 °C. After addition of an oil soluble initiator, polymerizations were carried out over night in an oil bath set at either 70 °C or 38 °C depending on the used initiator. The respective compositions of the dispersed phase and the types of initiators of the different reactions are summarized in Table 1.

After the polymerization, coagulates were removed by filtration and the resulting dispersions were centrifuged at 5000 rpm for 30 min to collect the particles. The supernatant was removed and replaced by cyclohexane. Redispersion was carried out using a vortex. To remove excess surfactant, the dispersions were further washed four times with cyclohexane, following the procedure described above. The purified dispersions of the MGs in cyclohexane were examined with regard to the particle size distributions by means of DLS and SEM. Freeze-drying yielded the crosslinked gel particles as white to slightly yellow colored powders. The freeze dried particles were swollen over night at 0.5% (w/v) in water at room temperature. Two additional washing steps by centrifugation at 14,000 rpm for 90 min and redispersion in deionized water were performed to remove the sol content, which consisted of unreacted monomer and crosslinker, soluble (noncrosslinked) polymers, and oligomers. The purified particles were freeze dried and redispersed in the respective media by simple swelling at room temperature for 6 h at the desired concentration.

Photolytic Degradation

Dispersions of purified nanogels in water (0.0625% w/v) were placed in a quartz cuvette and the sample temperature was adjusted to 37 °C using a brass heating mantle combined with a cryostat. Turbidity was measured in transmission by using a He-Ne laser emitting at $\lambda = 633$ nm. Irradiation was carried out on a 90° angle relative to the laser beam by using a UV-LED emitting at $\lambda = 365$ nm with an intensity of $I = 30$ mW/cm^2. Transmitted light intensity of the laser was measured by a photo diode combined with a GG-385 edge filter to block scattered UV light. After irradiation, the samples were diluted and the particle sizes were determined by DLS. In addition, the particle morphologies were investigated by SEM. For irradiation time-dependent measurements, samples were taken after fixed irradiation intervals. UV–vis spectra were recorded using plate reader, and particle sizes were determined from diluted samples by DLS.

Enzymatic Degradation and Subsequent Irradiation

Sample preparation and instrumentation were analogous to the photolytic degradation experiments. After temperature equilibration for 30 min to 37 °C, 10 μL of a dextranase solution in water (47% w/v) were added to dispersions of purified nanogels in water (0.0625% w/v; 3 mL) and the turbidity was monitored. After 6 h of enzymatic treatment, UV irradiation was carried out for 45 min.

CONCLUSIONS

In conclusion, a new system for potential enzymatic- and light-triggered release applications based on degradable nanogels was successfully developed. Realization of this concept was achieved with newly synthesized water soluble crosslinking molecules consisting of vinyl functionalized dextrans. In addition to the inherent enzymatic cleavability of the dextran backbone upon incubation with dextranase, light sensitivity was incorporated into the crosslinking structure by the covalent attachment of multiple radically polymerizable acrylate units via a photolabile linkers to the polysaccharide chains. The resulting Dex-PL-A structures are characterized by their good water solubility which—in combination with multiple vinyl groups per chain—offers the possibility for the preparation of a broad range of enzymatic- and light-degradable (nano-)gels by copolymerization with different vinyl functionalized monomers from aqueous solutions. As a first model system, AAm was copolymerized with Dex-PL-A in an inverse miniemulsion. High-crosslinking efficiency of the resulting p(AAm-*co*-Dex-PL-A) nanogels was achieved by systematic increasing the Dex-PL-A/AAm ratio. It was shown that irradiation with UV light induced either complete particle degradation or a desired specific DGS by adjusting the irradiation time accordingly. In addition, a two-step degradation profile based on the subsequent appliance of the two orthogonal stimuli was realized by first generating highly swollen nanogels by partial enzymatic cleavage of the Dex-PL-A crosslinking molecules and their successive complete degradation upon irradiation. The facile way of preparation at ambient temperatures of 37 °C from aqueous solutions and the observed low initial DGS is promising for the potential embedding of functional water soluble compounds already during the polymerization. In combination with the well-defined degradation profiles, this feature renders these new materials highly interesting for triggered release applications in aqueous dispersions.

D. Klinger acknowledges the International Max Planck Research School (IMPRS) for financial support.

REFERENCES AND NOTES

1 Nayak, S.; Lyon, L. A. *Angew. Chem. Int. Ed. Engl.* **2005,** *44*, 7686–7708.

2 Das, M.; Zhang, H.; Kumacheva, E. *Annu. Rev. Mater. Res.* **2006,** *36*, 117–142.

3 Lin, C. C.; Metters, A. T. *Adv. Drug Delivery Rev.* **2006,** *58*, 1379–1408.

4 Hendrickson, G. R.; Smith, M. H.; South, A. B.; Lyon, L. A. *Adv. Funct. Mater.* **2010,** *20*, 1697–1712.

5 Eichenbaum, G. M.; Kiser, P. F.; Shah, D.; Simon, S. A.; Needham, D. *Macromolecules* **1999,** *32*, 8996–9006.

6 Vinogradov, S. V.; Bronich, T. K.; Kabanov, A. V. *Adv. Drug Delivery Rev.* **2002,** *54*, 135–147.

7 Nayak, S.; Gan, D. J.; Serpe, M. J.; Lyon, L. A. *Small* **2005,** *1*, 416–421.

8 Nayak, S.; Lee, H.; Chmielewski, J.; Lyon, L. A. *J. Am. Chem. Soc.* **2004,** *126*, 10258–10259.

9 Eichenbaum, G. M.; Kiser, P. F.; Dobrynin, A. V.; Simon, S. A.; Needham, D. *Macromolecules* **1999,** *32*, 4867–4878.

10 Goh, S. L.; Murthy, N.; Xu, M. C.; Frechet, J. M. J. *Bioconjugate Chem.* **2004,** *15*, 467–474.

11 Murthy, N.; Thng, Y. X.; Schuck, S.; Xu, M. C.; Frechet, J. M. J. *J. Am. Chem. Soc.* **2002,** *124*, 12398–12399.

12 Bulmus, V.; Chan, Y.; Nguyen, Q.; Tran, H. L. *Macromol. Biosci.* **2007,** *7*, 446–455.

13 Jhaveri, S. B.; Carter, K. R. *Macromolecules* **2007,** *40*, 7874–7877.

14 Franssen, O.; vanOoijen, R. D.; deBoer, D.; Maes, R. A. A.; Herron, J. N.; Hennink, W. E. *Macromolecules* **1997,** *30*, 7408–7413.

15 Franssen, O.; van Ooijen, R. D.; de Boer, D.; Maes, R. A. A.; Hennink, W. E. *Macromolecules* **1999,** *32*, 2896–2902.

16 Abdurrahmanoglu, S.; Firat, Y. *J. Appl. Polym. Sci.* **2007,** *106*, 3565–3570.

17 Hennink, W. E.; Talsma, H.; Borchert, J. C. H.; DeSmedt, S. C.; Demeester, J. *J. Controlled Release* **1996,** *39*, 47–55.

18 Chiu, H. C.; Hsiue, G. H.; Lee, Y. P.; Huang, L. W. *J. Biomater. Sci. Polym. Ed.* **1999,** *10*, 591–608.

19 Franssen, O.; Stenekes, R. J. H.; Hennink, W. E. *J. Controlled Release* **1999,** *59*, 219–228.

20 vanDijkWolthuis, W. N. E.; Tsang, S. K. Y.; Kettenesvanden-Bosch, J. J.; Hennink, W. E. *Polymer* **1997,** *38*, 6235–6242.

21 vanDijkWolthuis, W. N. E.; vanSteenbergen, M. J.; Underberg, W. J. M.; Hennink, W. E. *J. Pharm. Sci.* **1997,** *86*, 413–417.

22 Franssen, O.; Vandervennet, L.; Roders, P.; Hennink, W. E. *J. Controlled Release* **1999,** *60*, 211–221.

23 De Geest, B. G.; De Koker, S.; Demeester, J.; De Smedt, S. C.; Hennink, W. E. *Polym. Chem.* **2010,** *1*, 137–148.

24 Kloxin, A. M.; Kasko, A. M.; Salinas, C. N.; Anseth, K. S. *Science* **2009,** *324*, 59–63.

25 Klinger, D.; Landfester, K. *Soft Matter* **2011,** *7*, 1426– 1440.

26 Piggott, A. M.; Karuso, P. *Tetrahedron Lett.* **2005,** *46*, 8241–8244.

27 Holmes, C. P.; Jones, D. G. *J. Org. Chem.* **1995,** *60*, 2318–2319.

28 Reichmanis, E.; Smith, B. C.; Gooden, R. *J. Polym. Sci. Part A: Polym. Chem.* **1985,** *23*, 1–8.

29 Alvarez, M.; Best, A.; Pradhan-Kadam, S.; Koynov, K.; Jonas, U.; Kreiter, M. *Adv. Mater.* **2008,** *20*, 4563–4567.

30 Klinger, D.; Aschenbrenner, E. M.; Weiss, C. K.; Landfester, K. *Polym. Chem.* **2012,** DOI: 10.1039/c1py00415h.

31 Buhler, S.; Lagoja, I.; Giegrich, H.; Stengele, K. P.; Pfleiderer, W. *Helv. Chim. Acta* **2004,** *87*, 620–659.

32 Barzynski, H.; Sanger, D. *Angew. Makromol. Chem.* **1981,** *93*, 131–141.

33 Landfester, K.; Musyanovych, A. In Chemical Design of Responsive Microgels. Pich, A. Richtering W., eds., Berlin Heidelberg: Springer; **2010; Vol.** *234*, pp 39–63.

34 Landfester, K. *Angew. Chem. Int. Ed. Engl.* **2009,** *48*, 4488–4507.

35 Landfester, K.; Willert, M.; Antonietti, M. *Macromolecules* **2000,** *33*, 2370–2376.

36 Al-Manasir, N.; Zhu, K. Z.; Kjoniksen, A. L.; Knudsen, K. D.; Karlsson, G.; Nystrom, B. *J. Phys. Chem. B* **2009,** *113*, 11115–11123.

37 Lecner, M. D. *J. Serb. Chem. Soc.* **2005,** *70*, 361–369.

38 Holmes, C. P. *J. Org. Chem.* **1997,** *62*, 2370–2380.